Korean J. Chem. Eng., **28**(3), 927-932 (2011)
DOI: 10.1007/s11814-010-0441-y

Sorptive removal and recovery of nickel(II) from an actual effluent of electroplating industry: Comparison between *Escherichia coli* biosorbent and Amberlite ion exchange resin

In Seob Kwak*, Sung Wook Won, Sun Beom Choi**, Juan Mao*, Sok Kim**, Bong Woo Chung*, and Yeoung-Sang Yun*,**,†**

*Department of Bioprocess Engineering and Department of BIN Fusion Technology, Chonbuk National University, Jeonbuk 561-756, Korea
**Division of Semiconductors and Chemical Engineering, Chonbuk National University, Jeonbuk 561-756, Korea
(*Received 10 June 2010 • accepted 1 October 2010*)

Abstract−The removal and recovery of nickel(II) from wastewater of an electroplating factory was investigated using the waste *Escherichia coli* biomass as the biosorbent. The results were compared with those from using Amberlite IRN-150 as a commercial sorbent resin. The resin showed better performance with a q_{max} value of 30.48 mg/g compared to 26.45 mg/g for the biomass, as predicted by the Langmuir isotherm model. Kinetic experiments revealed that the biosorption equilibrium was attained within 15 min. In the recycling of the sorbents, the desorption of nickel(II) from Amberlite was only 50%, which is too low for the adsorption performance of the resin to be maintained at an economic level in subsequent cycles. In contrast, the biomass exhibited reasonable adsorption-desorption performance over three repeated cycles. The capability for repeated use of the sorbent over several cycles and for recovery of the metal ions is the main advantage of the waste biomass.

Key words: Biosorption, Fermentation Waste, Resin, Nickel, Regeneration

INTRODUCTION

Enormous industrial activities have caused a massive release of pollutants into the environment. Among these pollutants, metals are particularly harmful due to their non-biodegradable nature, toxicity and cost. Nickel use is widespread with industrial processes such as electroplating, plastics manufacturing, nickel-cadmium batteries, fertilizers, pigments, mining and metallurgical, porcelain enameling, copper sulfate manufacture and steam-electric power plants being the major contributors of nickel to the environment [1,2]. Nickel is reported as a potent carcinogen leading to cancer in the lungs, nose, stomach and bone [3]. Acute nickel poisoning causes headache, dizziness, nausea and vomiting, chest pain, tightness of chest, dry cough, shortness of breath, rapid respiration, cyanosis and extreme weakness [4]. The nickel-containing effluents emanating from the aforementioned industries are highly toxic to both flora and fauna, and therefore require treatment prior to discharge. The main techniques utilized for the treatment of nickel(II)-bearing waste streams include precipitation, coagulation, evaporation, adsorption, ion exchange, membrane processing and solvent extraction [5-9]. However, the application of such processes is often restricted because of technical and/or economic constraints. In addition, these techniques mostly target the removal, but not recovery, of the metals from the wastewaters. Recovery is very important as it offers the potential to reduce operational costs and, more importantly, reduces the total nickel usage, thereby increasing the environmental safety.

Waste biomass production from fermentation industries has increased in recent years, making its disposal a central issue in developing countries such as Korea. Ocean dumping, landfill and incineration have been the most widely used methods for the waste biomass disposal. However, increasing environmental concerns have rendered these disposal techniques less attractive. Alternatively, fermentation wastes can be used for several applications, thereby increasing their value. Among the studies that have reported on the use of fermentation wastes for the removal of various metal pollutants [10], few have examined the use of *Escherichia coli* from L-phenylalanine (LPA) fermentation industries for the effective removal, recovery and subsequent reuse of metals from industrial wastewaters. Thus, we explored the possible utilization of fermentation waste (*E. coli*) as a biosorbent for the removal and recovery of nickel(II) ions from real wastewaters in batch mode operations and the subsequent reuse of the biosorbent in the next cycle.

EXPERIMENTAL SECTION

1. Adsorbents and Sorbate

Waste *E. coli* biomass from LPA production through fermentation was obtained from Daesang Corporation (Gunsan, Korea) in the form of a fine dry powder. They were ground and sieved to obtain particle sizes with diameter below 50 μm being selected for sorption studies. For comparison, sorption studies were also conducted with a commercial resin: Amberlite IRN-150 (Merck Ltd., brown and cream-colored spherical beads, exchange capacity: ≥0.6 mmol/mL (Anion), ≥0.7 mmol/mL (Cation) and particle size: 0.3-1.18 mm (≥95%). This is a strong acid H^+ form and strong basic OH^- form resin.

Nickel(II)-containing wastewater was collected from Samsung

†To whom correspondence should be addressed.
E-mail: ysyun@chonbuk.ac.kr

Table 1. The composition of nickel(II)-containing wastewater was collected from Samsung Electro-Mechanics Co. Ltd (Suwon, Korea)

Anion	Concentration (mg/L)	Cation	Concentration (mg/L)	pH
$NH_2SO_3^-$	9268.2	Na^+	0.3	6.52
Cl^-	168.2	NH_4^+	12.5	
SO_4^{2-}	508.6	[a]Ni^{2+}	2860	
NO_3^-	524.3			

[a]Ni^{2+} was measured by inductively coupled plasma-atomic emission spectrometry

Electro-Mechanics Co. Ltd (Suwon, Korea) in pre-cleaned, 5 L plastic containers. The ionic content of the collected wastewater was analyzed using ion chromatography (Metrohm, 792 Basic IC, Switzerland). The composition of the nickel(II)-containing wastewater is summarized in Table 1. All reagents, unless otherwise indicated, were of AnalaR grade and were purchased from Sigma-Aldrich.

2. Scanning Electron Micrograph (SEM) and Fourier Transform Infrared (FT-IR) Studies

The waste *E. coli* biomass used as adsorbent was coated with a thin layer of gold under vacuum and examined by scanning electron microscopy (SEM; JEOL, JSM-6400, Japan). The infrared spectrum of a biomass sample, prepared as a KBr disc, was analyzed with an FT-IR spectrometer (JASCO, FT/IR-4100, Japan) within the range 400-4,000 cm^{-1} to identify the functional groups responsible for the biosorption.

3. Batch Experiments

The pH edge experiments were carried out with a sorbent (0.3 g) which was brought into contact with 30 mL of nickel(II)-containing wastewater in a 50 mL, high-density polyethylene bottle. The pH of the solution was initially adjusted to the desired pH value and controlled using 0.1 M HCl or NaOH. The bottles were then shaken in an incubated rotary shaker at 160 rpm and 25 ºC. After equilibrium was attained, the supernatant was separated and analyzed for nickel concentration after appropriate dilution in inductively coupled plasma-atomic emission spectrometry (SHIMADZU, ICP-7510, Japan). To evaluate the sorption capacity of the sorbents, sorption isotherms experiments were conducted by bring into contact sorbents with 30 mL nickel(II)-containing wastewater. The mass of sorbents was altered from 5 to 100 g/L. The solution was controlled at pH 6 during the experiments. Kinetic experiments were carried out with a sorbent (2 g) which was brought into contact with 100 mL of nickel(II)-containing wastewater. The amounts of nickel(II) sorbed by the sorbents were calculated from the differences between the concentrations of nickel(II) added to that in the supernatant using the following equation:

$$Q_e = \frac{V(C_i - C_f)}{M} \quad (1)$$

where Q_e is the amount of nickel(II) uptake (mg/g), C_i and C_f the initial and final nickel(II) concentration in the solution (mg/L), respectively, V the solution volume and M is the mass of sorbents.

4. Models to Fit Batch Experimental Data

The following two equilibrium isotherm models were used to fit the experimental data:

$$\text{Langmuir model [11]: } Q = \frac{Q_{max} b C_e}{1 + b C_e} \quad (2)$$

$$\text{Freundlich model [12]: } Q = K_F C_e^{1/n} \quad (3)$$

where Q is the metal uptake (mg/g), C_e the equilibrium metal concentration (mg/L), Q_{max} the maximum metal uptake (mg/g), b the Langmuir equilibrium constant (L/mg), K_F the Freundlich constant (L/g), and n the Freundlich constant.

The experimental adsorption kinetic data were modeled using pseudo-first- and pseudo-second-order kinetics, and their non-linear forms are shown below as Eqs. (4) and (5), respectively [13,14]:

$$Q_t = Q_e(1 - \exp(-k_1 t)) \quad (4)$$

$$Q_t = \frac{Q_e^2 k_2 t}{1 + Q_e k_2 t} \quad (5)$$

where Q_e is the amount of nickel sorbed at equilibrium (mg/g), Q_t the amount of nickel sorbed at time t (mg/g), k_1 the first-order equilibrium rate constant (L/min) and k_2 the second-order equilibrium rate constant (g/(mg min)).

5. Regeneration Experiments

The same procedure as that employed in the sorption equilibrium experiments was used for the regeneration experiments. The metal-laden sorbent was separated by filtration and re-suspended in 30 mL of deionized water adjusted to pH 1.0 taken in a 50 mL plastic bottle. The bottles were then shaken in an incubated rotary shaker at 160 rpm and 25 ºC for 5 h. The sorbent was separated by filtration and the supernatant was analyzed for nickel, whereas the sorbent was reused for the next adsorption cycle. Several such sorption-desorption cycles were conducted to determine the reusability of the sorbent.

RESULTS AND DISCUSSION

1. SEM and FT-IR Analyses

The SEM images of the *E. coli* biomass are shown in Fig. 1 at ×700 and ×10,000 magnifications. The biomasses were spherical with various diameters of less than 50 μm (Fig. 1).

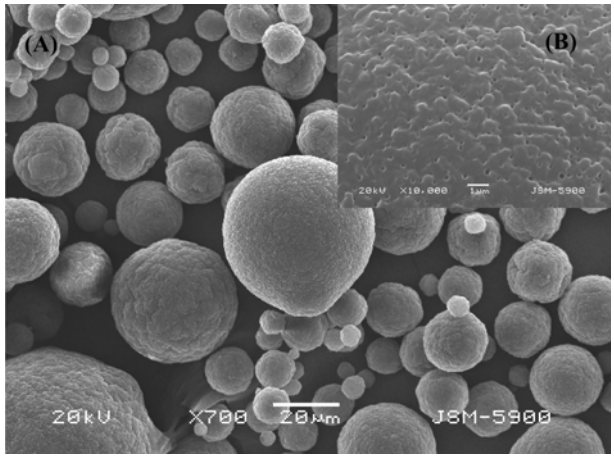

Fig. 1. SEM images of waste *E. coli* biomass surface. Magnification is (A) 700× and (B) 10,000×.

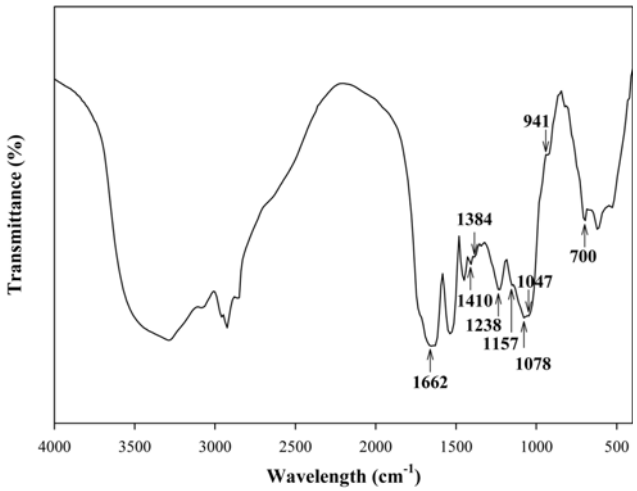

Fig. 2. FT-IR spectrum of waste *E. coli* biomass.

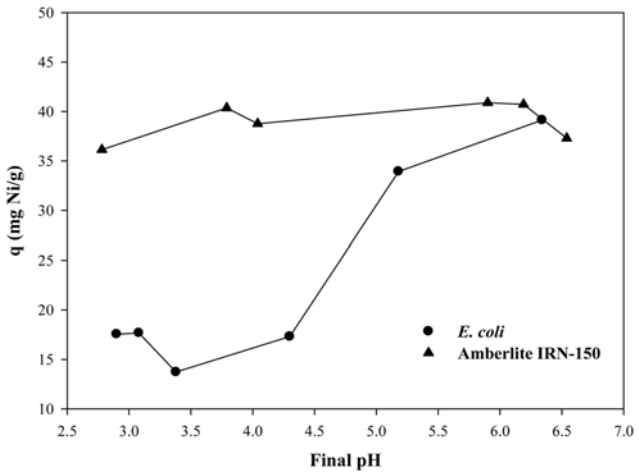

Fig. 3. The effect of solution pH on nickel(II) sorption. Initial nickel (II) concentration: 2,860 mg/L; Adsorbent dose: 10 g/L; Temperature: 25 °C.

To determine the main functional groups in the *E. coli* biomass, an FTIR study was conducted. The FTIR spectrum displays a number of absorption peaks, indicating the complex nature of the biomass (Fig. 2). The strong band at 3,800-2,500 cm^{-1} was attributed to -OH in the carboxyl group [15], the medium strength absorption peaks at 1,384 and 1,410 cm^{-1} to the symmetrical stretching of the carboxylate anion and carboxylic acid, respectively [16], and some other absorption bands to various bonds of a phosphonate group (P=O stretching at 1,157 cm^{-1}, P-OH stretching at 1,078 and 941 cm^{-1}, P-O-C stretching at 1,047 cm^{-1}) [16,17]. The FTIR spectrum of the biomass also showed some characteristic absorption bands of an amine group [18,19]: an N-H bending band at 1,662 cm^{-1}, N-H out of plane bending band near 700 cm^{-1}, and C-N stretching band at 1,238 cm^{-1}. No N-H stretching band in the range 3,500-3,300 cm^{-1} was visible, possibly having been obscured by the strong and large band of the carboxyl group within the range 3,800-2,500 cm^{-1}. To summarize, the FTIR spectrum of the *E. coli* biomass supported the presence of carboxyl, phosphonate, and amine groups. Positively charged pollutants such as nickel(II) could be bonded to the negative sites of the biomass such as carboxyl and phosphonate groups.

2. pH Edge

The pH edge experiments revealed that nickel(II) biosorption was significantly increased at pH above 5 in the waste biomass. In case of Amberlite resin, the uptake remained almost constant at all final pH between 2.5 and 6.5 (Fig. 3), likely because this is a strong acid and strong base type resin. The negatively charged functional groups on the biomass such as carboxyl and phosphonate can attract and bind positively charged nickel ions. The nickel(II) uptake was low at strong acidic conditions because of the competition between protons and nickel ions to occupy the binding sites. For instance, the pKa value of the carboxylic group was earlier identified as being with the range 3.8-5.0 [20]. Therefore, the carboxylic group is negatively charged at pHs higher than 5.0 and consequently attracts the positively charged nickel(II) ions. Control experiments reported by Vijayaraghavan et al. [21] show that nickel tends to precipitate at pH≥7. Considering the speciation, nickel exists only as nickel(II) ions in the pH range of 1-6, while the hydroxide form of nickel is

Table 2. Comparison between the nickel(II) uptake capacity of *E. coli* with other biosorbents reported in the literature

Biosorbents	Nickel(II) uptake (mg/g)	Operational conditions			Reference
		pH	C_i (mg/L)	M (g/L)	
Mucor rouxii	1.78	6	10	0.66	[23]
Non-living ureolytic culture	7.41	6	100	1	[24]
Deactivated protonated yeast	9.01	6.75	400	1	[25]
Living Ureolytic culture	12.58	6	100	1	[24]
Undaria pinnatifida	24.71	3-7	50	0.1-0.5	[26]
Anaerobic granular sludge	26	5	100	0.5	[27]
Activated sludge	40.6	5	400	1	[28]
S. cerevisiae	46.3	5	200	1	[29]
Penicillium chrysogenum	54.92	5.5	100	1	[30]
Chlorella sorokiniana	60.57	5	200	1	[31]
Ulva reticulata	62.3	4.5	109	2	[32]
E. coli	26.45	6	2860	5-100	Present study
Amberlite IRN-150	30.48	6	2860	5-100	Present study

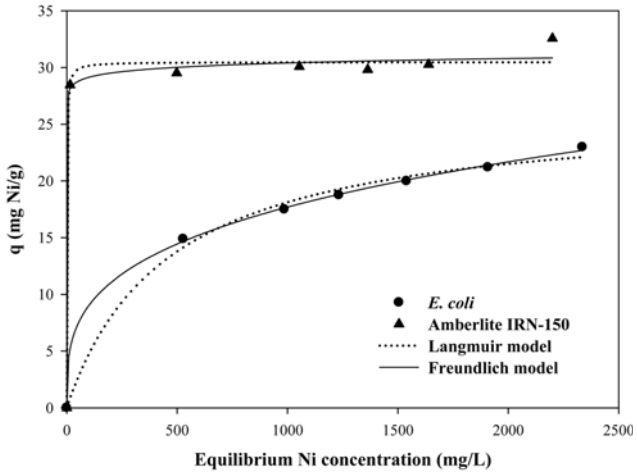

Fig. 4. Nickel(II) sorption isotherms at pH 6. Initial nickel(II) concentration: 2,860 mg/L; Adsorbent dose: 5-100 g/L; Temperature: 25 °C. The curves were predicted by the Langmuir (Dot) and Freundlich (Line) model.

initiated at pH greater than 6 [22]. Therefore, precipitation may also contribute to the nickel uptake at pH>6. The uptake of nickel(II) was consistently higher by the Amberlite resin than by the waste biomass (Fig. 3), which was attributed to the excess of nickel(II) ion-attracting, negatively charged groups in the resin. From Table 2, The nickel(II) uptake of *E. coli* was compared with other biosorbents reported in the literature. The nickel(II) uptake capacity showing the dependence on experimental conditions.

3. Isotherm and Kinetics

To evaluate the maximum biosorption potential of the waste *E. coli* biomass and Amberlite IRN-150 resin, isotherm experiments were conducted at pH 6.0 (Fig. 4). A typical H-shaped biosorption isotherm [33] was observed for the resin compared to an L-shaped biosorption isotherm for the waste *E. coli* biomass. The ratio between the nickel(II) concentration remaining in solution and that sorbed onto the solid decreased with increasing nickel(II) concentration, to produce a concave curve with a strict plateau. The Amberlite resin performed better than the waste biomass did. The Langmuir model incorporates two easily interpretable constants: Q_{max}, which corresponds to the maximum uptake the system can achieve; and b, which is related to the affinity between the sorbate and sorbent [11]. The former is often used to compare the performance of the biosorbent, while the latter characterizes the initial slope of the isotherm. Thus, a high Q_{max} (i.e., high Langmuir constant) and a steep initial isotherm slope (i.e., high b) are generally desirable for good biosorbents [34]. The maximum nickel uptakes were 26.45 and 30.48 mg/g, while the b values were 0.002 and 0.913 L/mg for the waste biomass and Amberlite resin, respectively. The correlation coefficient (R^2) values were greater than 0.993, whereas the percentage error values were less than 0.83% (Table 3). The Freundlich isotherm was originally empirical, but was later interpreted as sorption to heterogeneous surfaces or surfaces supporting sites of varied affinities. It is assumed that the stronger binding sites are occupied first and that the binding strength decreases with increasing degree of site occupation [12]. The maximum K_F and n values were both larger for the Amberlite resin than for the waste biomass, which implies that the binding capacity was greater and the affinity between the sorbent and sorbate was also higher than that of the waste *E. coli* biomass (Table 3).

Table 3. Sorption isotherm constants during nickel sorption by *E. coli* and Amberlite IRN-150. Initial nickel(II) concentration: 2,860 mg/L; adsorbent dose: 5-100 g/L; temperature: 25 °C

Isotherm models	Constants	*E. coli*	Amberlite IRN-150
Langmuir	Q_{max} (mg/g)	26.45	30.48
	b (L/mg)	0.002	0.913
	R^2	0.994	0.993
	ε (%)	0.83	0.02
Freundlich	K_F (L/g)	2.34	26.77
	n	3.41	54.28
	R^2	0.999	0.995
	ε (%)	0.23	0.19

The sorption kinetics is important in the treatment of wastewater, as it provides valuable insights into the reaction pathways and mechanisms of sorption reactions. Experimental kinetic data revealed that both the waste biomass and Amberlite resin showed a metal uptake of more than 95% in the first 15 min (Fig. 5). This was mainly due to the high affinity towards the metal and the presence and availability of active groups on the sorbent. The experimental biosorption kinetic data were modeled using a non-linear form of pseudo-first- and pseudo-second-order kinetics. In the former case, the correlation coefficients were above 0.966, and the calculated Q_e was close to the experimental Q_e, confirming the accuracy of the model prediction of the kinetic data for the present system. The equilibrium uptakes were predicted as 26.2 and 33.76 mg/g, compared to the experimental uptakes of 26.43 and 33.43 mg/g, for the waste biomass and Amberlite resin, respectively (Table 4). The slight differences in the Q_e values were attributed to a time lag, possibly as a result of a boundary layer or an external resistance controlling the beginning of the sorption process [35]. The pseudo-first-order rate

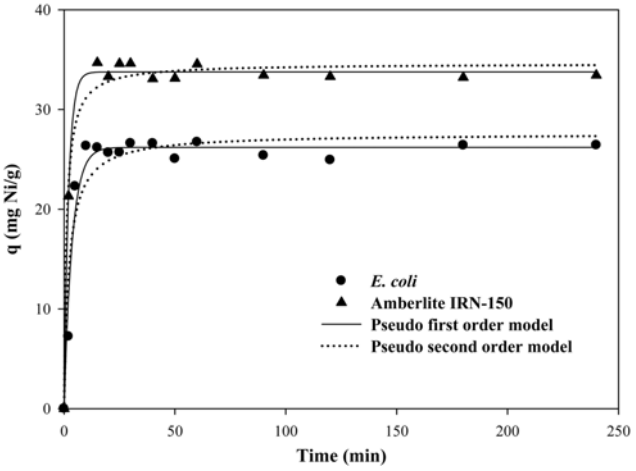

Fig. 5. Nickel(II) sorption kinetics at pH 6. Initial nickel(II) concentration: 2,860 mg/L; Adsorbent dose: 20 g/L; Temperature: 25 °C. The curves were predicted by the pseudo-first-order (Line) and pseudo-second-order (Dot) model.

Table 4. Biosorption kinetic constants for nickel biosorption. Initial nickel(II) concentration: 2,860 mg/L; adsorbent dose: 20 g/L; temperature: 25 °C

Kinetic models	Constants	*E. coli*	Amberlite IRN-150
	Q_e (mg/g) (exp.)	26.43	33.43
Pseudo-first-order	Q_e (mg/g)	26.20	33.76
	k_1 (L/min)	0.277	0.499
	R^2	0.966	0.996
	ε(%)	3.86	0.00
Pseudo-second-order	Q_e (mg/g)	27.58	34.61
	k_2 (g/(mg min)	0.017	0.026
	R^2	0.915	0.986
	ε(%)	5.86	0.39

constants were determined as 0.277 and 0.499 L/min for the waste biomass and Amberlite resin, respectively, which confirmed the faster adsorption rate of the Amberlite resin. In addition, the predicted curves showed good agreement with the experimental data (Fig. 5). The pseudo-second-order model is based on the sorption capacity of the solid phase. The correlation coefficients were reasonably close to those of the pseudo-first-order model (Table 4). However, the second-order model over-predicted the equilibrium uptake values as 27.58 and 34.61 mg/g, whereas the rate constants were determined as 0.017 and 0.026 g/mg min, for the waste biomass and Amberlite resin, respectively. Vijayaraghavan et al. [21] reported an equilibrium time of around 200 min by polysulfone-immobilized waste biomass of *Corynebacterium glutamicum* for nickel(II) removal from aqueous solutions, which is almost 10 times more than our result. Similarly, equilibrium was attained after 105 min in the use of carbonized maize cob and *Aspergillus japonicus* biomass for the removal of nickel(II) ions from electroplating industry effluent [2,36].

4. Metal Recovery and Regeneration of the Biosorbent

The ability to regenerate the biosorbent is a key factor for assessing the potential of the biosorbent for commercial applications [37]. In addition, a metal recovery capability enabling the reuse of the metal would confirm the superior efficiency of the biosorption technique over the existing methods. The pH edge experiments (Fig. 3) revealed that the H^+ ions occupied negatively charged groups under strongly acidic conditions and that very little metal uptake was recorded in the sorbents at pH below 5. This result implies that the sorbed nickel ions can be recovered by further reducing the pH values below 2 [21]. Experiments investigating the metal recovery and biosorbent regeneration were conducted to evaluate the possibility of recycling the biomass over several cycles. The nickel recovery and biosorbent regeneration for three consecutive adsorption-desorption cycles of the waste biomass and Amberlite resin are shown in Fig. 6. After the high efficiency of nickel(II) sorption and desorption in the first cycle of the waste biomass, the efficiency of both progressively declined in the subsequent batch cycles but with no consistent pattern. With the Amberlite resin, the nickel(II) ion desorption efficiency was only around 50% in the first cycle, thereby severely reducing both the metal recovery and the resin sorption efficiency in the consecutive cycles. This rendered the sorption process using the Amberlite resin more expensive than that using the waste biomass, despite the high sorption efficiency of the former towards nickel. To summarize for the waste biomass, desorption was maintained at around 80% after the third cycle, which was only a slight reduction from the level after the first cycle, while adsorption was reduced by only 5% from the first to third cycles. For the Amberlite resin, however, adsorption was reduced by around 30% between the first and third cycles. These results proved the superiority of the waste biomass for the sorption of nickel ions from industrial wastewaters.

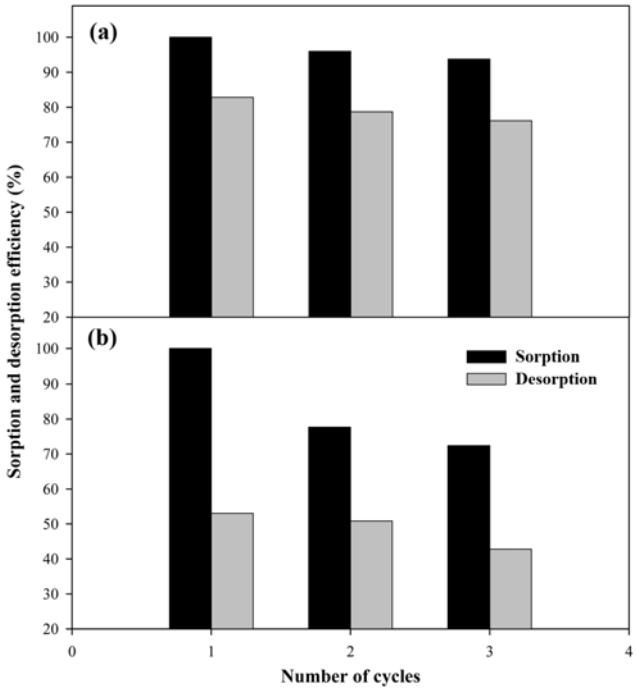

Fig. 6. Nickel(II) recovery and adsorbent regeneration at consecutive cycles: (a) waste *E. coli* biomass and (b) Amberlite IRN-150 resin.

CONCLUSION

The feasibility of utilizing *E. coli* biomass from fermentation wastes for the removal and recovery of nickel(II) ions from wastewaters has been confirmed by the results in the current study. The SEM images of the *E. coli* biomass confirmed that the biomass was spherically shaped with various diameters and plenty of groove-like structures. The pH edge studies showed that nickel(II) biosorption was significantly increased at pH above 5 for the waste biomass, whereas in the case of Amberlite resin, the uptake remained almost constant at all final pH between 2.5 and 6.5. Comparative studies on the adsorption capacity between the waste biomass and Amberlite IRN-150 resin demonstrated the slight superiority of the latter. The rapid attainment of equilibrium achieved by both sorbents confirmed their economic feasibility for industrial application. The waste biomass showed a better nickel recovery efficiency than the Amberlite resin in regeneration studies, thereby demonstrating its economy and environmental friendliness. These study results confirmed the economic and environmental sustainability of applying the freely available *E. coli* biomass sourced from fermentation wastes for the removal and

recovery of nickel(II) ions from industrial wastewater. Furthermore, the utilization of such fermentation waste avoids the serious environmental threat posed by its own disposal.

ACKNOWLEDGEMENTS

This work was supported by National Research Foundation of Korea Grant funded by the Korean Government (NRL 2009-0083194, WCU R31-2008-000-20029-0).

REFERENCES

1. B. Volesky and Z. R. Holan, *Biotechnol. Prog*., **11**, 235 (1995).
2. G. Selvakumari, M. Murugesan, S. Pattabi and M. Sathishkumar, *Bull. Environ. Contam. Toxicol*., **69**, 195 (2002).
3. A. L. Mukherjee, *Environmental Pollution and Health Hazards-causes and control*, Golgotia publications, New Delhi (1986).
4. S. P. Parker, *Encyclopedia of Environmental Science*, 2nd Ed. McGraw Hill, New York (1980).
5. A. Selatnia, A. Madani, M. Z. Bakhti, L. Kertous, Y. Mansouri and R. Yous, *Miner. Eng*., **17**, 903 (2004).
6. A. Papadopoulos, D. Fatta, K. Parperis, A. Mentzis, K. J. Haralambous and M. Loizidou, *Sep. Puri. Technol*., **39**, 181 (2004).
7. N. Bukhari, C. M. Ashraf and M. Mazhar, *J. Membr. Sci.*, **283**, 182 (2006).
8. A. Agrawal, M. K. Manoj, S. Kumari, D. Bagchi, V. Kumar and B. D. Pandey, *Miner. Eng*., **21**, 1126 (2008).
9. M. Tanaka, Y. Huang, T. Yahagi, M. K. Hossain, Y. Sato and H. Narita, *Sep. Purif. Technol*., **62**, 97 (2008).
10. P. R. Puranik and K. M. Paknikar, *J. Biotechnol*., **55**, 113 (1997).
11. I. Langmuir, *J. American Chem. Soc.*, **40**, 1361 (1918).
12. H. Freundlich, *J. Phys. Chem.*, **57**, 385 (1906).
13. S. Lagergren and B. K. Svenska, *Veterskapsakad Handlingar*., **24**, 1 (1898).
14. Y. S. Ho and G. McKay, *Process Biochem.*, **34**, 451 (1999).
15. R. N. Adeem, T. M. Ansari and A. M. Khalid, *J. Hazard. Mater.*, **156**, 64 (2008).
16. S. K. Das and A. K. Guha, *Colloid Surf. B*., **60**, 46 (2007).
17. F. Pagnanelli, M. P. Papini, L. Toro, M. Trifoni and F. Veglio, *Environ. Sci. Technol*., **34**, 2773 (2000).
18. G. C. Panda, S. K. Das and A. K. Guha, *Collod Surf. B*., **62**, 173 (2008).
19. S. W. Won, S. B. Choi and Y. S. Yun, *Biochem. Eng. J*., **28**, 208 (2006).
20. S. Schiewer and B.Volesky, *Biosorption processes for heavy metal removal, Environmental Microbe-Metal Interactions*, ASM Press, Washington DC (2002).
21. K. Vijayaraghavan, M. W. Lee and Y. S. Yun, *Biochem. Eng. J*., **41**, 228 (2008).
22. F. M. Doyle and Z. Liu, *J. Colloid Interf. Sci*., **258**, 396 (2003).
23. Y. Guangyu and V. Thiruvenkatachari, *Water Res*., **37**, 4486 (2003).
24. I. Mustafa, *Colloid Surf. B*., **62**, 97 (2008).
25. V. Padmavathy, *Bioresour. Technol*., **99**, 3100 (2008).
26. C. Zhen, M. Wei and H. Mei, *J. Hazard. Mater*., **155**, 327 (2008).
27. H. H. Alaa and N. M. Catherine, *Bioresour. Technol*., **97**, 692 (2006).
28. Z. A. Qodah, *Desalination*., **196**, 164 (2006).
29. O. Ayla and O. Dursun, *J. Hazard. Mater*., **100**, 219 (2003).
30. S. Deng and Y. P. Ting, *Water Res*., **39**, 2167 (2005).
31. H. N. Catherine, V. Bohumil and C. Daniel, *Water Res*., **41**, 2473 (2007).
32. K. Vijayaraghavan, *Clean*., **36**, 3, 299 (2008).
33. G. Limousin, J. P. Gaudet, L. Charletm, S. Szenknect, V. Barthes and M. Krimissa, *Appl. Geochem*., **22**, 249 (2007).
34. Y. S. Ho, J. F. Porter and G. McKay, *Water Air Soil Poll*., **141**, 1 (2002).
35. G. McKay, Y. S. Ho and J. C. P. Ng, *Sep. Purif. Meth*., **28**, 87 (1999).
36. A. R. Binupriya, M. Sathishkumar, K. Swaminathan, E. S. Jeong, S. E. Yun and S. Pattabi, *Bull. Environ. Contam. Toxicol*., **77**, 219 (2006).
37. M. Iqbal and A. Saeed, *Process Biochem*., **42**, 148 (2007).